Aerosol and Air Quality Research, 18: 1617–1630, 2018

ISSN: 1680-8584 print / 2071-1409 online
doi: 10.4209/aaqr.2017.11.0492

Field Measurements for Quantifying Semi-Volatile Aerosol Influence on Physical and Optical Properties of Ambient Aerosols in the Kathmandu Valley, Nepal

Sujan Shrestha[1,2], Siva Praveen Puppala[1*], Bhupesh Adhikary[1], Kundan Lal Shrestha[2], Arnico K. Panday[1]**

[1] *International Centre for Integrated Mountain Development (ICIMOD), Khumaltar, Lalitpur, Nepal*
[2] *Kathmandu University, Department of Environmental Science and Engineering, Dhulikhel, Kavre, Nepal*

ABSTRACT

An intensive field campaign was conducted during the pre-monsoon season of 2015 in the urban atmosphere of the Kathmandu Valley to study the influence of the semi-volatile aerosol fraction on physical and optical properties of aerosols. Ambient air was siphoned through a specific ambient air inlet and then split into two parts. The first part connected directly with an ambient air sample while the second received the air sample through a thermodenuder (TDD). The aerosol properties, such as the aerosol number, size distribution, absorption, and scattering, were studied using Condensation Particle Counters (CPCs), Scanning Mobility Particle Sizers (SMPSs), Aethalometers (AE33) and Nephelometers, respectively. The differences in the properties of the aerosol fraction at room temperature and other TDD set temperatures (50°C, 100°C, 150°C, 200°C, 250°C, and 300°C) were calculated to study the influence of the semi-volatile aerosol fraction on ambient aerosols. The evaporated fraction of the semi-volatile aerosols increased with the TDD set temperature. The semi-volatile fraction of the aerosol number increased from 16% to 49% of ambient aerosol, while the peak mobility diameter of particles shifted from around 60 nm to 40 nm as the temperature increased from 50°C to 300°C. However, increasing the TDD set temperature had no influence on the effective diameter of the aerosol size distribution. Larger aerosol size bins of the SMPS experienced a significantly stronger influence (~70%) from temperature increments compared to smaller size bins (~20%). The semi-volatile aerosol fraction amplified BC absorption by up to 28%, while scattering by the semi-volatile aerosol fraction contributed up to 71% of the total.

Keywords: Aerosol number concentration; Absorption; Scattering; Black carbon.

INTRODUCTION

Aerosols are suspended particles in the air that are solid, liquid, or a mixture of both states, ranging in size from a few nanometers to several micrometers (Ehhalt *et al.*, 1999; Warneck, 1999). Studies have shown that aerosols have profound effects on the climate (Pöschl, 2005), human health (Kampa and Castanas, 2008; Mauderly and Chow, 2008), and visibility in the atmosphere (Dzubay *et al.*, 1982). Atmospheric aerosols are among the key factors that influence the earth's radiative energy balance. Aerosols affect the climate directly by absorbing and scattering incoming solar radiation (Haywood and Shine, 1997; Yu *et al.*, 2006) and indirectly by acting as cloud condensation nuclei and affecting the optical properties and life cycles of cloud (Ishizaka and Adhikari, 2003).

Aerosols are classified as primary or secondary depending upon their origin. Primary aerosols are particles that are emitted directly from the combustion of fossil fuels and biomass, such as black carbon as well as sea salts and windblown mineral dust. Secondary aerosols are formed due to condensation, oxidation and chemical transformation (Seinfeld and Pandis, 2006). Secondary aerosols tend to be semi-volatile in nature (Hennigan *et al.*, 2008). The aerosol components that do not condense under normal atmospheric conditions are considered as volatile aerosols, while those aerosols that remain in a condensed phase under certain atmospheric conditions are classified as semi-volatile. Although the non-volatile aerosols have negligible vapor pressure and remain in a condensed phase under normal atmospheric conditions (Fuzzi *et al.*, 2006), semi-volatile aerosols are believed to contribute most significantly to the toxicity of particles (Stevanovic *et al.*, 2015). The volatility of an aerosol provides an indication about its emission sources, history, and chemical composition (Capes *et al.*,

* Corresponding author.
Tel.: +977-1-5003222 ext. 163
E-mail address: SivaPraveen.Puppala@icimod.org
** Corresponding author.
Tel.: +12544000797
E-mail address: sujanshrestha101@gmail.com

2008). The semi-volatile fraction of an aerosol largely depends on the source of aerosol generation and the atmospheric conditions around the sampling site (Robinson *et al.*, 2007).

Past field and laboratory measurements show that the volatility of aerosols is largely influenced by reaction temperature and precursor gases. Previous studies show that a large fraction of aerosols is highly volatile under 150°C (Ishizaka and Adhikari, 2003; Murugavel and Chate, 2011 and references therein). Measurements made by Lee *et al.* (2010) and Murugavel and Chate (2011) indicate that the semi-volatile fraction in ambient aerosol was between 50% and 80% of the number concentration. Lin (2013) reported that the potential radiative effect of secondary organic aerosols (SOA), which are a major fraction of semi-volatile aerosols, on climate was around one third of total aerosols. Chung and Seinfield (2002) reported that organic carbon (OC) has a global radiative forcing of –0.09 to –0.17 Wm^{-2} wherein 50% of the radiative forcing is contributed by SOA. The above studies show that semi-volatile aerosols play a significant role in the air quality and energy budget from local to global scales.

Various epidemiological studies have reported the impact of semi-volatile aerosols on human health (Ronai *et al.*, 1994; Dalton *et al.*, 2001; Huang *et al.*, 2014; Lerner *et al.*, 2014; Sarigiannis *et al.*, 2015). Some of these studies find that in higher concentrations these semi-volatile aerosols can act as potential carcinogens. For example, the semi-volatile polycyclic aromatic hydrocarbons (PAHs) are not just carcinogenic but also cause genetic susceptibility and oncogene activation (Ronai *et al.*, 1994). Exposure to semi-volatile components, such as dioxins, induces heart disease leading towards mortality (Dalton *et al.*, 2001). These studies point toward the need for critical assessment of the semi-volatile aerosol fraction, which can lend better understanding of human health end points.

Studies on source apportionment of the ambient air in the Kathmandu Valley based on Non-methane Volatile Organic Compounds (NMVOCs) indicate that brick kilns (~10%), traffic (~17%), residential biofuel and waste disposal (~11%), and industries (32%) are the major sources of pollution (Sarkar *et al.*, 2017). Similar findings but with a slight variation in percentages were also observed when estimating the sources of EC and OC from PM_{10} (Kim *et al.*, 2015), PAHs from TSP (Chen *et al.*, 2015), $PM_{2.5}$ and bulk aerosol studies (Shakya *et al.*, 2017, 2010). Although none of the studies quantified the contribution of the semi-volatile aerosol fraction to the ambient atmosphere directly. Source apportionment studies of $PM_{2.5}$ and PM_{10} within the valley indicate a ~50% contribution from semi-volatile aerosols composed primarily of OC, NH_4, and SO_4. This fraction, however, varies from time to time, depending upon the sampling period and sampling method. In this context, it is important to study the impact of the semi-volatile aerosols on physical and optical properties of aerosols in the Kathmandu Valley. To the best of our knowledge, this is the first study of its kind in this area.

EXPERIMENTAL SITE AND GENERAL METEROLOGY

The Kathmandu Valley (Fig. S1(a)) sits 1,300 m above mean sea level and is surrounded by hills as high as 2,500 m, as shown in Fig. 1(b). We conducted our experiments to characterize the semi-volatile fraction of aerosols contributing to the particulates of the valley. Experiments were conducted on the rooftop of the Integrated Centre for International Mountain Development (ICIMOD) headquarters in Lalitpur, Nepal (27.6464°N, 85.3235°E). As shown in Fig. S1(b), the sampling site is located 7 km southwest of the city center. The sampling site is primarily surrounded by residential dwellings, hospitals, educational institutes, and brick kilns (the nearest brick kiln is 2 km). There are no obstructions around the sampling site within a 50 m radius. During the measurement period, instruments sampled ambient air from an inlet located 2 m above the roof of a four-story building (~15 m above the ground).

The general meteorology in Kathmandu during the observation period (https://www.wunderground.com/) included a mean temperature of 21.8 ± 3.1°C and average relative humidity of 75 ± 10.2%. The daily average wind speed was approximately 1.3 m s^{-1}, indicating the prevalence of light air conditions during the sampling time period. The dominant wind direction during this period was westerly (south west–north west) and easterly (south east–north east) due to the presence of high mountain peaks on the northern and southern fringes of the Kathmandu Valley (Panday *et al.*, 2009b; Regmi and Maharjan, 2015). Atmospheric pressure was also observed to be ~868 hPa. In these weather conditions, all measurements were carried out within the span of a few months (Table S1). Care was taken so that no experiments were conducted during the occasional rain events.

EXPERIMENTAL SETUP

The measurements presented in this study were made during the pre-monsoon season of 2015. The total duration of sample collection was approximately 1,470 hours. This collection period included approximately 490 hours of both CPC and Aethalometer experiments, 470 hours of nephelometer experiments, and 20 hours of SMPS experiments.

To use a single Thermodenuder (TDD) instrument, we arranged sets of experiments with different instrument pairs that were run sequentially. Our experimental setup consisted of an ambient air inlet split into two sets of identical sampling instruments. We used a waterproof total suspended particulate assembly with a debris screen (Met One Instruments, Inc, USA) to protect the inlet from bugs and insects. The inlet was regularly cleaned, and the O-ring in the TSP inlet was lubricated. The first set of instruments was connected directly to an ambient sample inlet, and the second set received air from the sample inlet after passing through the Thermodenuder (TDD). A schematic diagram of the instrumental setup is shown in Fig. S2.

Four sets of experiments were conducted with this setup, using four different pairs of instruments to explain aerosol

properties with ambient conditions, with the loss of the semi-volatile fraction and the impact of the difference. A similar approach has been used in previous studies as well (Stanier *et al.*, 2004; Huffman *et al.*, 2008; Lack *et al.*, 2012). Because the TDD flow rate is restricted to 3 L min^{-1}, we could not connect multiple instruments to maintain the TDD flow rate. In each experiment, the TDD's temperature was changed over time to examine the fractional loss of the semi-volatile aerosol fraction at increasing temperatures. A summary of the four sets of the experimental setup and respective sampling dates is provided in Table S1.

We note that the experiments had to be halted due to a massive earthquake in Nepal, a period lasting from late April till late May. In the preceding sections, the term "wet sample" is used to refer to ambient measurements, while the term "heated sample" refers to measurements carried out with instruments coupled with the TDD. TDD temperatures were set to room temperature, 50°C, 100°C, 150°C, 200°C, 250°C, and 300°C in experiments 1, 3, and 4. Similar experimental temperatures were used in previous studies (Ishizaka and Adhikari, 2003; Jennings *et al.*, 1994; Murugavel and Chate, 2011). In addition, there will not be much particle loss when aerosols are dried without heating, for example, when aerosols are dried using Nafion dryers. This has been tested, and such new generations of aerosol drying systems have been used widely in aerosol research in labs as well as in the field (Stanier *et al.*, 2004; Grover *et al.*, 2005; Grimm and Eatough, 2009). In experiment 2, we examined only the relationship between particle size and volatility at room temperature, 50°C, 100°C, 200°C, and 300°C. All the equipment used in this study was brand new and factory-calibrated.

Instrument Description

The TDD used in this experiment is a Low-Flow (4 L min^{-1}) Thermodenuder Model 3065, manufactured by Topas GmbH, Germany (Madl *et al.*, 2003). The TDD consists of two sections: one for desorption and the other for adsorption. The TDD removes the semi-volatile fraction of an ambient sample by thermal desorption using a heating element. The semi-volatile fraction that is evaporated by thermal desorption is then adsorbed by the activated carbon, which is used as the working material in the adsorption section. We operated the TDD only up to 300°C, though the instrument has the capacity to work at temperatures up to 400°C. The activated carbon was changed regularly to ensure an optimal working state for the instrument.

The Condensation Particle Counters (CPC) used in this study were Model 3775, manufactured by TSI Inc., USA. This instrument can detect particles as small as 4 nm in diameter and a wide range from 0 to 10^7 particles per cm^3. The CPC was operated with a flow rate of 1.5 L min^{-1}. Butanol was used as the working fluid, and the instrument was used in the auto drain mode. The efficiency and operation of the CPC Model 3775 have been further discussed by Hermann *et al.* (2007).

We operated a Scanning Mobility Particle Sizer (SMPS 3034, TSI Inc., USA) to measure the size distribution of aerosol particles. The SMPS 3034 works by separating fine particles within a range from 10 to 487 nm based on their electrical mobility. The SMPS 3034 is a compact instrument with inbuilt Differential Mobility Size Analyzer (DMA) and Condensation Particle Counter (CPC). The aerosol sampler pump has a flow rate of 1 L min^{-1}, and the sheath air flow of the DMA is 4 L min^{-1}. Since the sheath air flow is used just as a part of the feedback circuit maintaining constant flow, only 1 L min^{-1} of aerosol sample is passed through the SMPS via the TDD setup. We used a Neutralizer Model Number 308701, which is X-ray based. The operation of the SMPS 3034 has been further discussed by Hogrefe *et al.* (2006).

We used a Magee Scientific Aethalometer model AE33 to study the black carbon (BC) concentration and aerosol absorption in this study. During the entire measurement period, the maximum attenuation limit was set to 100. The instrument was operated at a flow rate of 2 L min^{-1}. The Aethalometer model AE33 measures BC concentration at seven different wavelengths (Drinovec *et al.*, 2015) using filter-based light attenuation due to aerosol loading. The manufacturer calibrated instrument measured light attenuation with soot particle loading. However, in real conditions, the light attenuation reported by the instrument represents all absorbing aerosols, including dust, BC, and organic carbon. Light absorbing organic aerosols are also known as brown carbon (Andreae and Gelencser, 2006; Bahadur *et al.*, 2012). We followed the methodology described by Drinovec *et al.* (2015) to convert BC concentration to absorption by using the relationship: BC Absorption in mm^{-1} = BC (in ng m^{-3}) $\times 10^{-3} \times$ MAC (the mass absorption cross sectional values). MAC values for the specific wavelengths are given by Drinovec *et al.* (2015). The absorption at the 880 nm wavelength is usually represented by BC absorption, as other particles such as dust and organic carbon do not absorb or their contribution to absorption is negligible at this wavelength (Singh *et al.*, 2014). However, at the 370 nm wavelength, aerosol absorption is represented by all three particle types—BC, organic carbon, and dust (Lim *et al.*, 2014).

We employed a TSI integrating Nephelometer 3563 to measure the aerosol scattering coefficient at three different wavelengths: 450 nm, 550 nm, and 700 nm. We followed the correction methodology given by Anderson and Ogren (1998). A Nephelometer records both total scattering and backscattering coefficients; however, we only report the results from total scattering. We operated the instruments for 24 hours at all previously reported TDD set temperatures. We followed the methodology explained by Anderson and Ogren (1998) to minimize angular truncation error in the dataset using the relationship: $\sigma_{corrected}$ = Correction factor (C) $\times \sigma_{neph}$ where C is the correction factor, σ_{neph} is the scattering coefficient reported by the instrument, and $\sigma_{corrected}$ is the corrected scattering coefficient.

Quality Control

Prior to the experiments, we conducted collocated intercomparison studies to estimate any biases within each set of identical instruments. Instruments were operated with a single inlet using a Y connector for a 24-hour period

with a 1-minute time resolution. Thereafter, correlations between the identical instruments were calculated. The slope was approximately equal to 1, and the r^2 values, to 0.99. No correction factors were required (see Fig. S3).

We conducted leakage tests on the inlet pipelines and the TDD. The main inlet (Fig. S2) was connected to a High Efficiency Particulate Arrestance (HEPA) filter to verify any leakage in the sampling system. HEPA filters are known to be highly efficient for producing zero aerosol concentration, removing a minimum of 99.7% of contaminants larger than 0.3 microns (MIL-STD-282 method 102.9.1). During the beginning of each set of experiments, a HEPA filter was connected to the main inlet to check for any leakages in the setup. When the HEPA filter was connected, particle concentration readings in both the identical instruments dropped to zero, as shown in Fig. S5. These tests gave us confidence that the instrument setup was proper and that there were no leaks in the system.

RESULTS AND DISCUSSION

The experimental results are summarized according to the aerosol number concentration, size distribution, and optical properties in this section.

Influence of Volatility on Aerosol Number Concentration

As discussed above, the influence of the semi-volatile aerosol fraction on the aerosol number concentration was identified using the CPC and CPC-TDD setup. During the first experiment, the TDD operated at room temperature by not providing power to the TDD thermal desorption section, as TDD works with only set as opposed to ambient temperatures. This setup provided information about the semi-volatile aerosol fraction loss due to the dry activated carbon column in the TDD. Activated carbon in the adsorption section of the TDD changes the equilibrium state of the semi-volatile aerosol fraction and leads to some evaporation, even at room temperature (Huffman *et al.*, 2009). We observed a 12% contribution to particle loss from the semi-volatile aerosol fraction at room temperature. Similar losses of 10% to 15% have also been reported in previous experiments (Fierz *et al.*, 2007; Lee *et al.*, 2010; Stevanovic *et al.*, 2015). These particle losses are governed by various other factors that cannot be completely avoided, such as sedimentation in micro-sized particles, as explained by Burtscher *et al.* (2001), and thermophoretic and diffusional loss in submicron particles, as detailed by Stevanovic *et al.* (2015).

The CPC and CPC-TDD setups shown in Fig. S2 operated for 24 hours at each set temperature. The comparison between wet and heated particle number concentrations at the set temperatures of 50°C and 300°C are shown in Fig. 1(a). The slope of the scatter plot gives the fraction of heated particles at a given temperature. We can see in Fig. 1(a) that there was a 16% and 49% particle loss at 50°C and 300°C, respectively. Kim *et al.* (2015) have also reported an increase in volatilization ratio with the increase in temperature in the characterization of semi-volatile ions study using a denuder. A strong correlation between wet and heated CPC indicates that the fractions of the semi-volatile aerosols at different ambient particle concentrations are similar. However, Fig. 1(a) also shows that the correlation between wet and heated becomes weaker when the ambient particle number concentration is very high (> 50000 # cm^{-3}). Similar wet and heated particle number comparisons were obtained at the other TDD set temperatures between 50°C and 300°C, and these are provided in Fig. 1(b). Fig. 1(b) also shows the temperature dependence of the semi-volatile

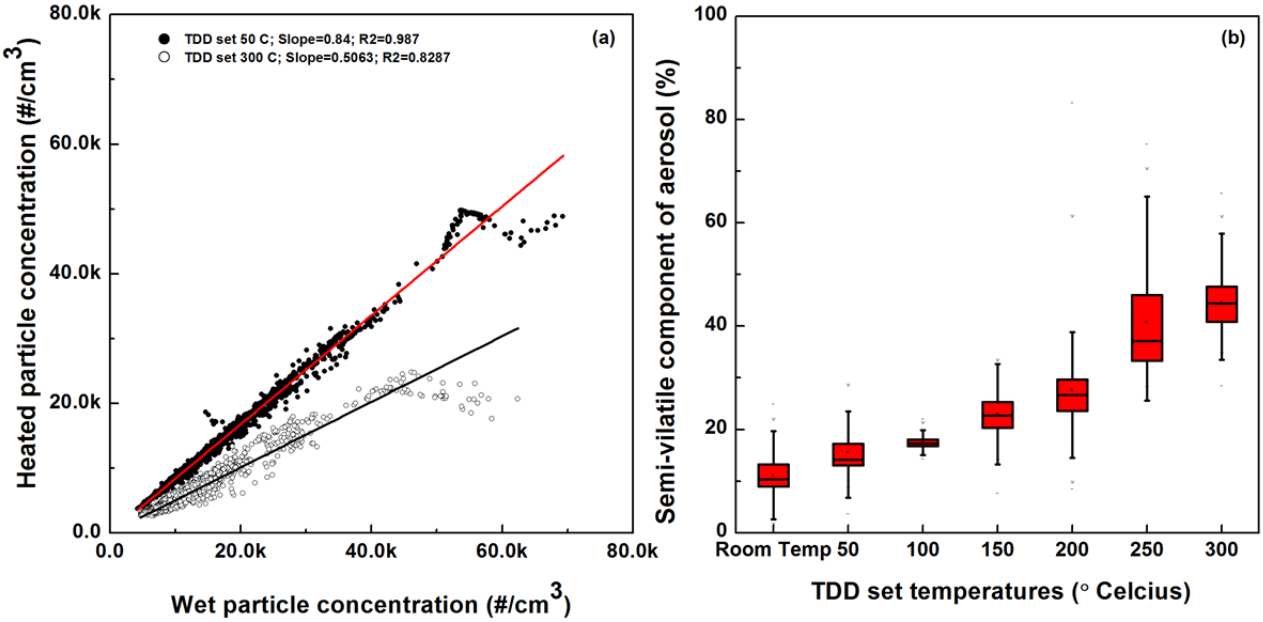

Fig. 1. (a) Comparison of wet versus heated particle concentration measured from CPC. Solid red and black lines indicate the slope of linear regression analysis for TDD set temperatures for 50°C and 300°C respectively, (b) Boxplot of the measured semi-volatile fraction of aerosols at different TDD set temperatures.

fraction of aerosols. Using 1-minute data, we calculated the particle percentage loss in heated sampling, displayed in the box plots. The semi-volatile aerosol number fraction was observed to be 12%, 16%, 18%, 23%, 28%, 46%, and 49% at room temperature, 50°C, 100°C, 150°C, 200°C, 250°C, and 300°C, respectively (Table S2).

Comparing these findings with other studies, we note that Murugavel and Chate (2011) reported from Pune, India, that at temperatures below 150°C, 51%–71% of the particles evaporated from the ambient aerosol. They also reported a 13%–26% loss between 150°C–300°C and a 7%–13% loss of particles at temperatures greater than 300°C. These results show that the evaporated fraction of the semi-volatile aerosols in different temperature ranges is comparatively less in Kathmandu than Pune. Although Murugavel and Chate (2011) used a SMPS for their study, we used a CPC for this study, which measures particle number concentrations from 4 nm to a few microns. The SMPS used by Murugavel and Chate (2011) only measures particle number concentrations between 10 nm and 487 nm. Kathmandu and Pune have different source characteristics, topography, and local meteorological conditions. Thus, these differences in the results from Murugavel and Chate (2011) should not be surprising.

We compared the semi-volatile aerosol fraction from our experiment with the standard chemical compounds that have evaporating temperatures equivalent to the TDD set temperatures. This comparison provides vital information about the aerosol chemical composition and volatility. A similar comparison technique has been adopted by several others studying this topic (Burtscher *et al.*, 2001; Ishizaka and Adhikari, 2003; Murugavel and Chate, 2011).

For further analysis, we sorted aerosol volatility into two categories: (I) highly volatile for those components that vaporize at temperatures ≤ 150°C and (II) moderately volatile for those that vaporize between 150°C and 300°C. We found 23% of the aerosols in our study to be highly volatile and 26% to be moderately volatile. The average aerosol number concentration during our experimental period was 16,136 # cm^{-3}. Out of this number, 2,038 # cm^{-3} are highly volatile in nature. These particles may represent some of the highly volatile aerosol components cited in Ishizaka and Adhikari (2003), such as ammonium chloride, ammonium sulphate, terpene, organic nitrogen, ethyl benzene, and sulfuric acid. Among the moderately volatile components cited in Ishizaka and Adhikari (2003), including diesel exhaust and ammonium bisulphate, we found 6319 # cm^{-3} aerosol particles to be moderately volatile in nature. In experiments carried out by Ishizaka and Adhikari (2003) and Shrestha *et al.* (2014), the remaining particles that did not volatilize up to 300°C were soot carbon, polymerized organic compounds, calcium carbonate, sea salt, and mineral dust, which may represent non-volatile aerosols in our experiment. Characterizing aerosol volatility as a function of chemical composition in the Kathmandu Valley needs further investigation.

The diurnal variation in wet and heated aerosol number concentrations and the semi-volatile aerosol fraction at 50°C and 300°C are shown in Fig. 2. We show results from only these two temperatures to represent the minimum and maximum TDD set temperatures. Results from other TDD set temperatures lie between these two temperature results. Figs. 2(a) and 2(b) shows the diurnal variation in wet aerosol number concentrations, which shows one peak during morning hours around 9 a.m. and another during evening hours around 8 p.m. Like other polluted cities, the Kathmandu Valley also exhibits rush hour peak emissions in the morning and the nighttime. Higher traffic density, emissions from indoor/cooking activities, and open garbage burning contributes the most. In addition, the lower Planetary Boundary Layer during these times also causes the accumulation of pollutants in the lower atmosphere. Particle number concentration is one of the primary indicators that reveals these activities. Hence, we observed peaks in the particle number concentration at around 9:00 and 20:00. Previous studies have also reported similar results (Panday and Prinn, 2009; Panday *et al.*, 2009a; Putero *et al.*, 2015).

Figs. 2(c) and 2(d) shows the semi-volatile aerosol number fraction at TDD set temperatures of 50°C and 300°C. The semi-volatile aerosol fraction did not show any diurnal variation like wet aerosols at 50°C, which indicates that the semi-volatile aerosol number fraction was uniform throughout the sampling period. However, as shown in Fig. 2(d) at the TDD set temperature 300°C, the semi-volatile aerosol fraction fluctuates with minor spikes. These spikes may represent different air masses or fresh nearby sources. Thus, the semi-volatile aerosol number fraction is significantly higher during peak events. However, compared to the aerosol number diurnal variation, the semi-volatile aerosol fraction does not exhibit strong diurnal variation (Fig. 2), and the fraction remains almost constant (Fig. 1).

By comparing the diurnal variations in the highly and moderately volatile aerosol fractions, we noticed the highly volatile aerosol contribution was nearly consistent throughout the day, while the moderately volatile aerosol fraction changed significantly during peak events (Fig. S6). As mentioned above, diesel combustion is a moderately volatile aerosol source, and this combustion (primarily from vehicle traffic) may account for the minor spikes in the semi-volatile aerosol fraction.

Influence of Volatility on Aerosol Size Distribution

Our experimental setup using the SMPS was different from other instrumental setups. In the first experiment using CPC, we identified that the semi-volatile aerosol number fraction did not show any strong diurnal variation. From this point, we wanted to understand particle size loss due to the semi-volatile aerosol fraction rather than diurnal variability. Hence, we operated identical SMPSs (as described in the instrument setup section) but changed the TDD set temperature every hour. We readily acknowledge that this decision also reveals a limitation of our study.

The results of the SMPS measurements are summarized in Table S2. The semi-volatile aerosol fraction was observed to be 62% and 49% during the SMPS and CPC experiments, respectively, at a TDD set temperature of 300°C (see Table S2). Similar behavior was seen at other temperatures as well. One possible reason for the difference

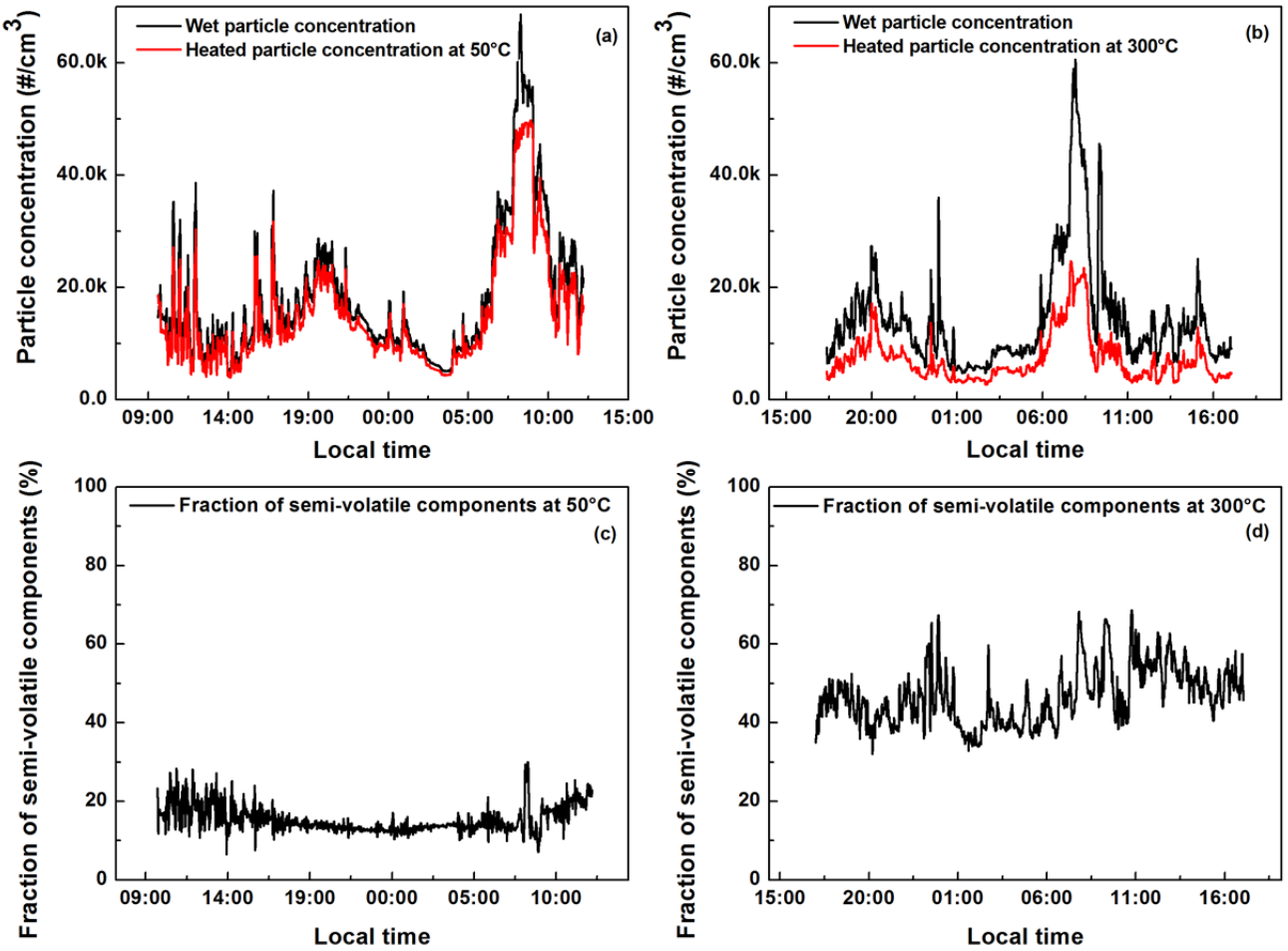

Fig. 2. Comparison of diurnal variation in particle number concentration of wet and heated aerosol at TDD set temperatures of (a) 50°C and (b) 300°C. Diurnal variation in fraction of heated particles at TDD set of temperatures (c) 50°C and (d) 300°C.

between the two measurements might be that the CPC reported aerosol number concentrations from 4 nm to a few microns, whereas the SMPS only monitors a range from 10 nm to 487 nm. The semi-volatile aerosol fraction may be higher in smaller diameter particles compared to larger diameter particles (Clarke, 1993; Burtscher *et al.*, 2001). Fig. 3 shows the number size distribution for the TDD at room temperature and 300°C. Even though the heated aerosol number size distribution at room temperature was significantly lower compared to wet aerosol, the peak mobility diameter did not shift significantly (from 85 nm to 80 nm). A similar comparison at 300°C shows a different result. At this temperature, the peak diameter shifted from approximately 60 nm to 40 nm. This correlates with a previous study (An *et al.*, 2007) that reported that when individual ammonium sulphate particles of different sizes evaporated at different temperatures, the particle sizes decreased significantly. With the increase in the TDD set temperatures, the non-volatile fraction of the aerosol composition does not experience any change, but the highly volatile or semi-volatile aerosols partially or completely evaporate, depending upon the implied temperature. This causes the size of the particles to shrink. As the TDD set temperature was increased, the fraction of the highly volatile and semi-volatile aerosols, which are either internally mixed or condensed over the less-volatile aerosols, also increased. Hence, the peak diameter of the aerosol shifts towards the smaller diameter relative to the TDD set temperature. A similar method has been used to separate and verify the presence of volatile aerosols in vehicular and aircraft exhaust as well as obsolete and study the extremely low volatile carbonaceous aerosols (Ferry *et al.*, 1999; Orsini *et al.*, 1999; Schmid *et al.*, 2002; Philippin *et al.*, 2004). Thus, we hypothesize that the decrease in the particle size of individual components of aerosol contributed in the shift in peak diameter towards a smaller diameter, as observed in our study.

In Fig. 4, we show individual size bin semi-volatile aerosol fraction loss as a function of the particle diameter at all experimental temperatures. The data show a greater reduction in aerosol size for larger diameter aerosols compared to smaller diameter aerosols. This may be due to the fact that the semi-volatile aerosol fraction at larger diameters may be in the form of a coating or internally-mixed state (Lang-Yona *et al.*, 2010). By losing this fraction, the aerosol size is expected to decrease. This conclusion is corroborated by the observation that as the size of the aerosols decreases, the peak diameter also shifts towards smaller diameters at

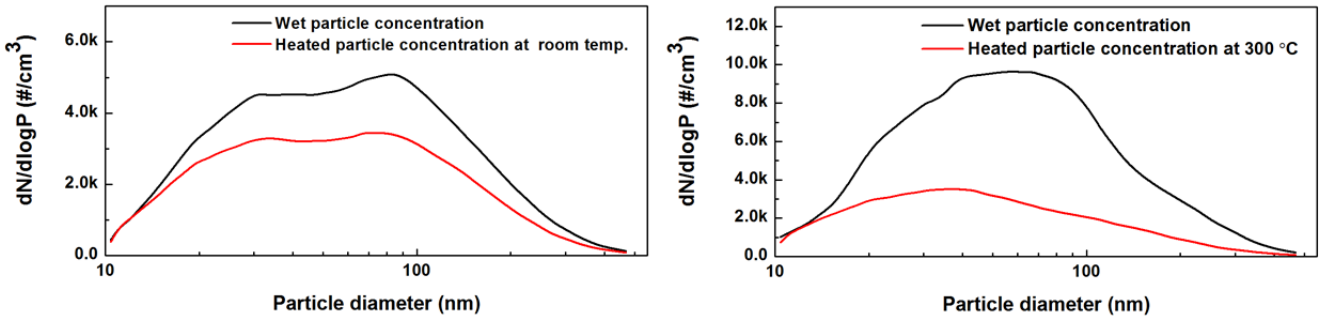

Fig. 3. Particle size distribution of wet and heated aerosol at (a) room temperature and (b) 300°C.

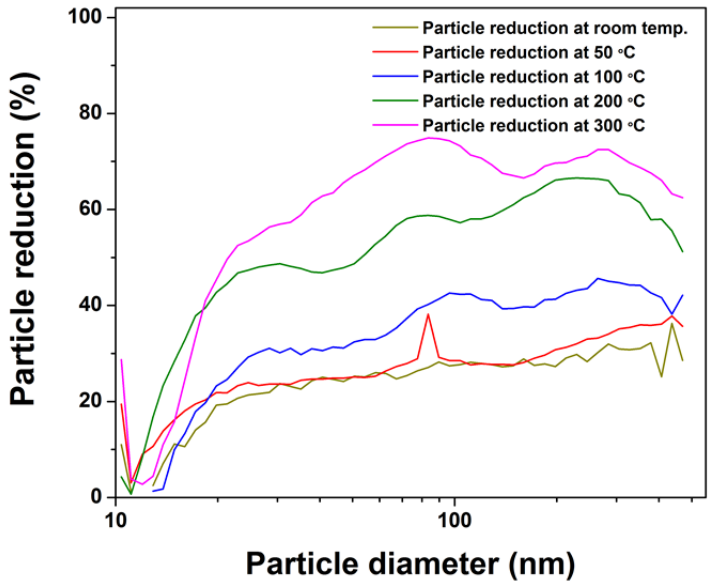

Fig. 4. Percentage of particle reduction from wet aerosol in their respective size bins at different TDD set temperatures.

higher temperatures. The shift in peak diameter was observed to be approximately 5–7 nm between wet and heated sampling at TDD set temperatures ≤ 100°C and shifted significantly to 20–22 nm at TDD set temperatures between 200°C and 300°C. Murugavel and Chate (2011) reported a variable particle loss percentage at different sizes and at different TDD temperatures over a year-long study. The difference between their study and ours may be attributed to differences in data collection. Murugavel and Chate (2011) reported data that represents monthly and annual averages, whereas our present study represents an event sampling (1 hour). Our results show that the mixing processes of ambient aerosols with highly and moderately volatile aerosols/precursors are different due to differing emission sources and require further investigation.

Influence of Volatility on Aerosol Absorption

In actual atmospheric conditions, BC exists in both elemental and mixed states. An Aethalometer-derived aerosol absorption represents both these states. Previous studies show that a non-absorbing material coating over elemental carbon (EC) enhances absorption due to the lensing effect (Schnaiter *et al.*, 2005; Zhang *et al.*, 2008; Lack and Cappa, 2010; Shiraiwa *et al.*, 2010). By removing this coating, the elemental carbon absorption will change. Dust aerosol displays absorption features in the ultraviolet (UV) through the VIS wavelengths due to its mineralogical composition; however, dust aerosol is non-volatile in nature. Elemental carbon (EC) and black carbon (BC) are operationally defined based on the measurement techniques. EC is exclusively a pure form of carbon, which is measured using thermal protocol utilizing different temperature profiles to separate it from organic carbon, whereas BC in the ambient air is an internal mix of the EC, dust, and organics condensed on it and is measured by the optical-attenuation method (Bond and Bergstrom, 2006; Snyder and Schauer, 2007; Petzold *et al.*, 2013). The optical-attenuation method used by the Aethalometer gives the measure of the light absorption and estimates BC concentration. However, this method cannot exactly estimate EC, as it is influenced by the aerosol mixing state and their chemical composition, and there is no unique conversion factor between light attenuation and EC concentration in ambient aerosol (Andreae and Gelencsér, 2006). In addition, EC can be volatilized above 600°C (Shrestha *et al.*, 2014), but below 300°C it is stable. In our study, semi-volatile aerosol fraction absorption is represented either by light absorbing organics or material (organic/inorganic) coated on EC.

Dust absorption is generally low in the spectral regime above 600 nm or tends to have a constant background absorption value for wavelengths longer than 600 nm (Gillespie and Lindberg, 1992; Lindberg *et al.*, 1993; Sokolik and Toon, 1999; Cao *et al.*, 2005; Kumar *et al.*, 2008). Hence, the wet and the heated absorption measured by the aethalometer at the 880 nm wavelength is representative of either EC or the mixed state of EC absorption (Lack and Cappa, 2010). The comparison of the wet and the heated aerosol absorption at 880 nm for 50°C and 300°C is shown in Fig. 5(a). The semi-volatile aerosol fraction absorption contribution to the total aerosol absorption was observed to be 20% and 28% at 50°C and 300°C, respectively, at the 880 nm wavelength. The loss of absorption from 50°C to 300°C increased only 8%, which is less than the particle loss of 33%. The particle loss was not proportional to the absorption loss at the 880 nm wavelength mainly due to EC and its mixed state. Since EC and dust cannot be volatilized under 300°C, the measured semi-volatile aerosol fraction absorption contribution at 880 nm is mainly from the EC mixed state with the semi-volatile aerosol fraction.

The highly and moderately volatile aerosol fraction contributed 21% and 7%, respectively, to aerosol absorption at the 880 nm wavelength. As shown in Table 1, one fourth of the aerosol absorption at the 880 nm wavelength was contributed by the semi-volatile aerosol fraction. The wet and the heated aerosol absorption at 370 nm is shown in Fig. 5(b). The semi-volatile aerosol fraction absorption was slightly higher at 370 nm compared to 880 nm (Table 1). The correlation for the wet and the heated absorption at both wavelengths stays similar at a higher range, unlike aerosol number concentrations reported by the CPC in the above sections. Results for other TDD set temperatures are summarized in Table 1.

If we assume BC mixing state absorption effects are similar at the 370 nm and 880 nm wavelengths, then the difference between 370 nm and 880 nm wavelength absorption may be attributed to changes in the intrinsic properties of the semi-volatile aerosols, the size of the aerosols, the mixing state, or brown carbon (BrC), which is unknown at present. This brown carbon- and intrinsic property-contributed absorption is approximately 3% and 9% at 50°C and

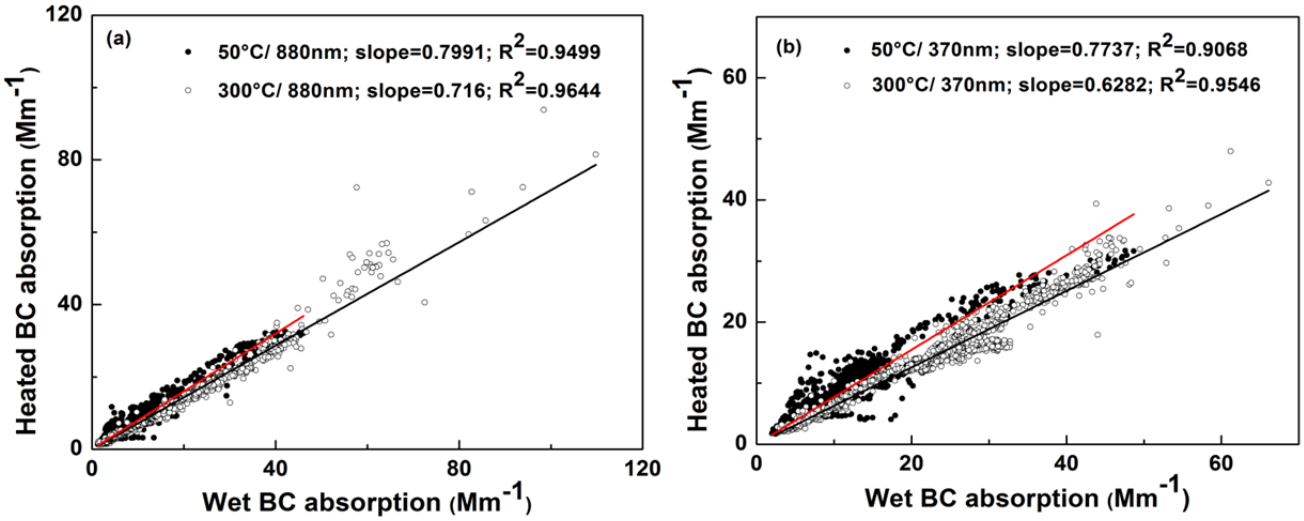

Fig. 5. Comparison of heated and wet BC absorption at TDD set temperatures of 50°C and 300°C at wavelengths (a) 880 nm and (b) 370 nm.

Table 1. Summary of influence of volatility on absorption at various temperatures.

TDD set temp. in °C	Loss of absorption at 370 nm (%) [a]	Loss of absorption at 880 nm (%) [a]	Absorption due to intrinsic properties, variation in size and brown carbon	Average absorption angstrom coefficient of wet aerosol [b] (Avg ± SD)	Average absorption angstrom coefficient of heated aerosol [b] (Avg ± SD)
Room temp.	16	16	0	1.02 ± 0.24	1.01 ± 0.24
50	23	20	3	1.08 ± 0.17	1.08 ± 0.18
100	19	18	1	1.01 ± 0.23	0.98 ± 0.23
150	25	21	4	0.97 ± 0.27	0.92 ± 0.30
200	31	27	4	0.97 ± 0.19	0.92 ± 0.18
250	35	28	7	1.03 ± 0.20	0.99 ± 0.22
300	37	28	9	1.30 ± 0.30	1.24 ± 0.30

[a] Average absorption Angstrom coefficient of wet aerosols (ambient aerosol) while the simultaneous heated experiment was being conducted at TDD set temperatures.
[b] The fraction represented in the table are derived from linear interpolation of slopes.

300°C, respectively. As shown in Table 1, the highly volatile aerosol fraction does not enhance the aerosol absorption at shorter wavelengths (0–3%). This finding indicates that highly volatile aerosols are not truly representative of brown carbon and intrinsic properties of the semi-volatile aerosols. Furthermore, as our results show, the moderately volatile aerosol fraction absorption is enhanced by 4–9% at 370 nm compared to 880 nm. This indicates that brown carbon and the intrinsic properties of the semi-volatile aerosols are moderately volatile in nature. We conclude that the brown carbon and intrinsic properties of the semi-volatile aerosol contribution are relatively less (0–9%) than the absorption enhancement (16–28%) due to the EC mixing state with the semi-volatile fraction of aerosols (Table 1).

In Figs. 6(a) and 6(b), we report the diurnal variation in absorption using the Aethalometer and the Aethalometer coupled with a TDD setup at 50°C and 300°C, respectively, for the 520 nm wavelength. As expected, both figures show an increase in BC absorption during the early morning hours, less absorption during the afternoon, and then an increase again toward evening—a finding similar to results in Backman *et al.* (2012). Fig. 6(c) shows that at 50°C, both the wet and the heated aerosol absorption demonstrate a similar magnitude as well as diurnal variation. The semi-volatile aerosol fraction absorption is approximately 20% at a TDD set temperature of 50°C. However, as shown in Fig. 6(d), although the diurnal variability is similar at 300°C, the semi-volatile aerosol absorption increases to nearly 30%. Unlike the CPC testing, the semi-volatile aerosol absorption is more variable throughout the day at a TDD set temperature of 50°C. It is also noteworthy that the semi-volatile aerosol absorption shows a similar variability at both TDD set temperatures.

Further, the data obtained from the Aethalometer were used to illuminate the wavelength dependency of the absorption, which is usually expressed as an Absorption Angstrom Exponent (AAE). AAE is simply the negative slope of the log of absorption by the log of two different wavelengths. In past studies, AAE has been used to make inferences about the dominant composition of absorbing aerosols in the atmosphere (Bergstrom *et al.*, 2007). Several studies report AAE values close to 1 for fossil fuel sources and close to 2 for biomass sources (Kirchstetter *et al.*, 2004). We computed AAE over a range of wavelengths (370 nm–970 nm) for the wet and the heated aerosol fraction individually (Table 1). Our results, as summarized in Table 1, show the wet aerosol AAE ranges from 0.97 to 1.30 with a median value around 1, implying the sampled aerosols are dominated by fossil fuel sources. The AAE results for 300°C, shown in Fig. 9, were around 1.5, indicating the influence of biomass burning sources.

Influence of Volatility on Aerosol Scattering

In this section, we discuss the influence of volatility on the scattering properties of the aerosols. As shown in Fig. 7(a), the semi-volatile aerosol fraction scattering contribution at the 700 nm wavelength was observed to be 8% and 66% of the wet aerosol scattering at the TDD set temperatures of 50°C and 300°C, respectively, whereas at the 450 nm wavelength, the semi-volatile aerosol fraction scattering contribution increased to 17% and 71% at the TDD set temperatures of 50°C and 300°C, respectively (Fig. 7(b)). The influence of wavelength on the scattering loss is evident for all set temperatures (Table 2). Even though the

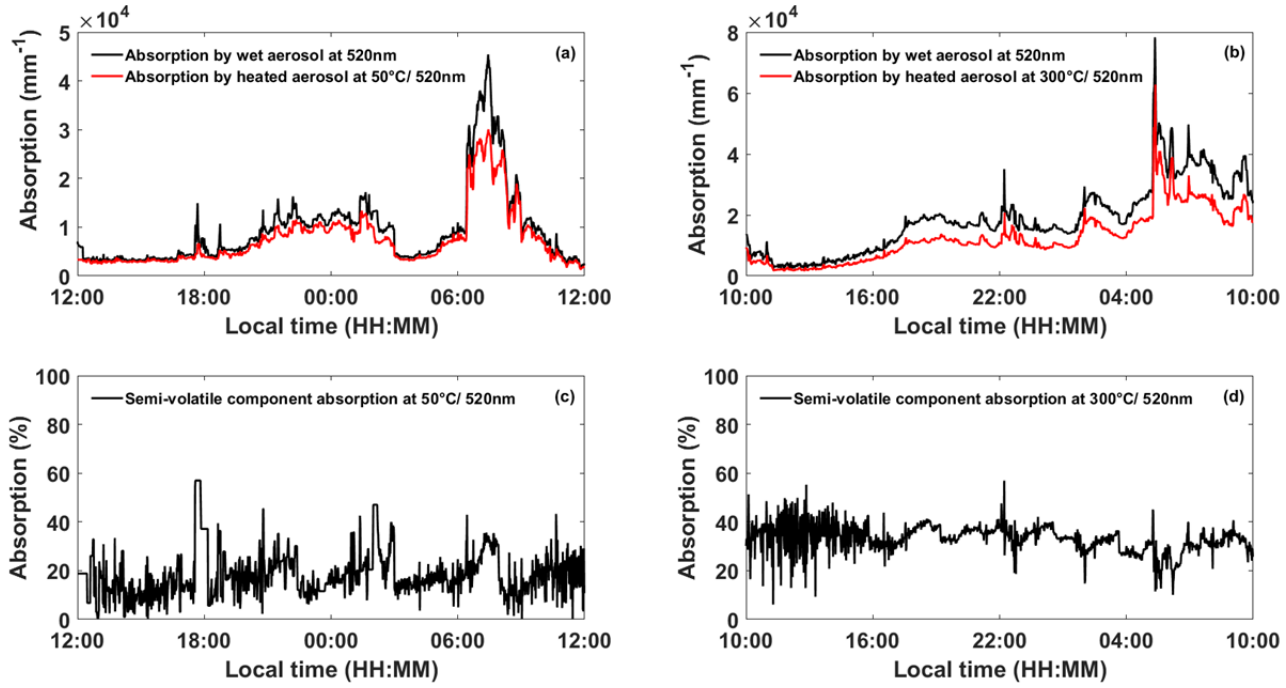

Fig. 6. Comparison of wet and heated aerosol absorption diurnal variation at 520 nm wavelength for TDD set temperatures of (a) 50°C and (b) 300°C. Diurnal variation in semi-volatile aerosol absorption fraction at 520 nm wavelength for TDD set temperatures of (c) 50°C and (d) 300°C.

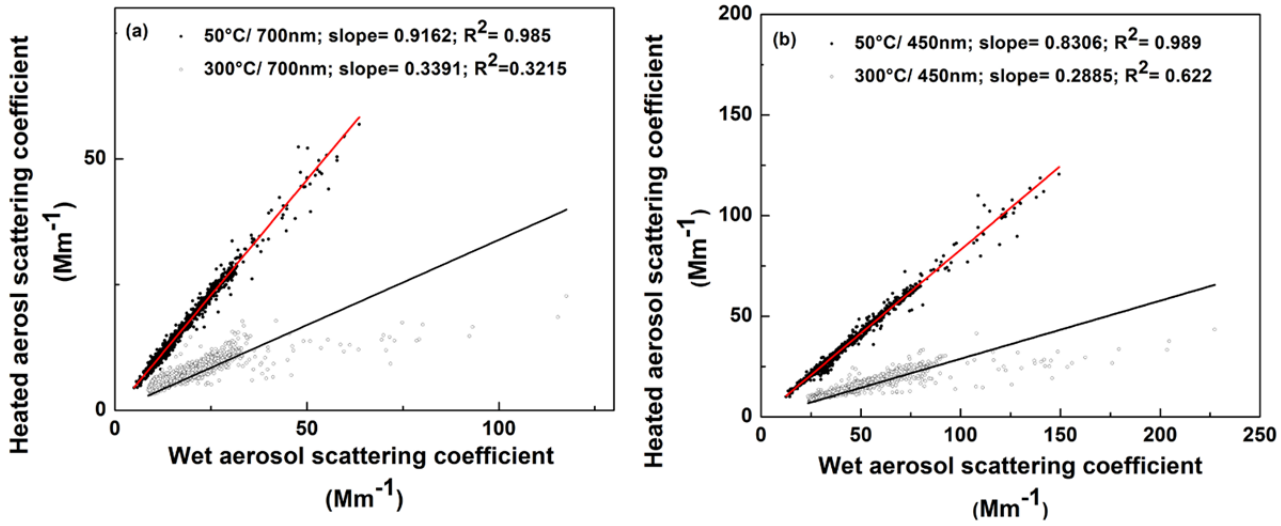

Fig. 7. Comparison of wet versus heated scattering coefficient at TDD set temperatures of 50°C and 300°C at wavelengths (a) 700 nm and (b) 450 nm.

Table 2. Summary of influence of volatility on scattering at various temperatures.

TDD set temp. in °C	Loss of scattering at 450 nm (%) [a]	Loss of scattering at 550 nm (%) [a]	Loss of scattering at 700 nm (%) [a]	Average scattering Angstrom coefficient of wet aerosol [b] (Avg ± SD)	Average scattering Angstrom coefficient of heated aerosol [b] (Avg ± SD)
Room temp.	18	15	8	1.94 ± 0.45	1.68 ± 0.45
50	17	13	8	1.76 ± 0.38	1.47 ± 0.34
100	29	27	20	1.92 ± 0.42	1.69 ± 0.39
150	39	38	32	1.96 ± 0.44	1.70 ± 0.44
200	48	46	40	1.93 ± 0.42	1.59 ± 0.40
250	62	59	52	1.94 ± 0.44	1.45 ± 0.41
300	71	70	66	1.99 ± 0.46	1.49 ± 0.41

[a] Average absorption Angstrom coefficient of wet aerosols (ambient aerosol) while the simultaneous heated experiment was being conducted at TDD set temperatures.
[b] The fraction represented in the table are derived from linear interpolation of slopes.

CPC and scattering experiments were conducted on different days, by assuming the urban air mass characteristics remain similar, we infer that the particle loss is not proportional to the scattering loss (Figs. 1(a), 7(a) and 7(b)). However, the scattering loss at the 700 nm wavelength is somewhat similar (66% to 62% versus 66% to 49%) to the particle loss in the SMPS experiment (Table S2 and Table 2). Thus, the smaller particle semi-volatile aerosol fraction has a greater influence on the total aerosol scattering. More tests are required to statistically validate these inferences. We summarize the results for all three wavelengths (450 nm, 550 nm, and 700 nm) at different TDD set temperatures in Table 2. Diurnal variability of the wet and the heated aerosol scattering (figure not shown) was observed to be similar to the CPC experiment. Using the methodology described in the above section, we also computed the Scattering Angstrom Exponent (SAE) (Table 2). The SAE of the wet and the heated aerosols observed in our study is within the range of the atmospheric aerosol Angstrom Exponent reported by previous studies (Bergstrom *et al.*, 2007; Cazorla *et al.*, 2013; Valenzuela *et al.*, 2015). Similar SAE values of the corresponding wet aerosol at different TDD set temperatures suggest that the studied aerosol had a similar composition throughout the study duration. The heated SAE value slightly increases with an increase in the TDD set temperature up to 150°, suggesting a decrease in the aerosol size (Bergstrom *et al.*, 2007). However, our results show that with a further increase in the TDD set temperatures, the SAE value decreased, which needs further investigation.

CONCLUSION

The present study provides the first information on quantifying the semi-volatile aerosol fraction influence on aerosol physical and optical properties over the Kathmandu Valley, a polluted site in the Hindu Kush Himalayan region of Nepal. Experimental results show that the semi-volatile aerosol number fraction ranged from 12% to 49% at TDD set temperatures from room temperature to 300°C, respectively. Our experiments suggest that highly volatile aerosols do not exhibit diurnal variability. However, the contribution of moderately volatile aerosols increases during peak

concentration events. In addition, SMPS experiment results show that the reduction in the aerosol size was high for larger diameter aerosols compared to smaller diameter aerosols due to the removal of the semi-volatile aerosol fraction. We also noted that the semi-volatile aerosol fraction mixing state contributed around 20% to total aerosol absorption. Aerosol absorption by the semi-volatile aerosol fraction was observed to be between 16% and 28% at the 880 nm wavelength, whereas the calculated brown carbon contribution to aerosol absorption ranged from 0 to 9%. The scattering contribution was observed to be in the range 18%–71% and 8%–66% at 450 nm and 700 nm, respectively. Our results show that the semi-volatile aerosol fraction contribution to aerosol scattering was significantly higher compared to the aerosol absorption and number. Since the scattering contribution of the semi-volatile aerosol fraction was found to be two times higher than its absorption, we infer that removing the semi-volatile aerosols will lead to a more absorbent atmosphere.

In short, our study shows that the semi-volatile aerosols play an important role in characterizing aerosol physical and optical properties over the Kathmandu Valley, which will further aid in understanding the health and climate impacts of aerosols. The results discussed are based on a limited and unique aerosol sampling in the Kathmandu Valley and can be improved to better characterize aerosols in the region.

ACKNOWLEDGEMENT

This project was partially funded by core funds of ICIMOD contributed by the government of Afghanistan, Australia, Austria, Bangladesh, Bhutan, China, India, Myanmar, Nepal, Norway, Pakistan, Switzerland, and the United Kingdom. We thank Pradeep Dangol for his technical support during initial instrument setup. The first author is also grateful to the Department of Environmental Science and Engineering, Kathmandu University for encouragement in carrying out this study. The views and interpretations in this publication are those of the authors and are not necessarily attributable to ICIMOD. We would like to acknowledge Dr. Parth Sarathi Mahapatra for scientific editing of the manuscript. Acknowledgements are also due to Dr. Christopher Butler for his English editing of the manuscript. We would also like to acknowledge the help of anonymous reviewers for helping us improve the quality of the manuscript and handling editor, Professor RenJian Zhang, for smooth handling of the manuscript.

SUPPLEMENTARY MATERIAL

Supplementary data associated with this article can be found in the online version at http://www.aaqr.org.

REFERENCES

An, W.J., Pathak, R.K., Lee, B. and Pandis, S.N. (2007). Aerosol volatility measurement using an improved thermodenuder: Application to secondary organic aerosol. *J. Aerosol Sci.* 38: 305–314.

Anderson, T.L. and Ogren, J.A. (1998). Determining aerosol radiative properties using the TSI 3563 integrating nephelometer. *Aerosol Sci. Technol.* 29: 57–69.

Andreae, M.O. and Gelencsér, A. (2006). Black carbon or brown carbon? The nature of light-absorbing carbonaceous aerosols. *Atmos. Chem. Phys.* 6: 3419–3463.

Backman, J., Rizzo, L.V., Hakala, J., Nieminen, T., Manninen, H.E., Morais, F., Aalto, P.P., Siivola, E., Carbone, S., Hillamo, R., Artaxo, P., Virkkula, A., Petäjä, T. and Kulmala, M. (2012). On the diurnal cycle of urban aerosols, black carbon and the occurrence of new particle formation events in springtime São Paulo, Brazil. *Atmos. Chem. Phys.* 12: 11733–11751.

Bahadur, R., Praveen, P.S., Xu, Y. and Ramanathan, V. (2012). Solar absorption by elemental and brown carbon determined from spectral observations. *Proc. Natl. Acad. Sci. U.S.A.* 109: 17366–17371.

Bergstrom, R.W., Pilewskie, P., Russell, P.B., Redemann, J., Bond, T.C., Quinn, P.K. and Sierau, B. (2007). Spectral absorption properties of atmospheric aerosols. *Atmos. Chem. Phys.* 7: 5937–5943.

Bond, T.C. and Bergstrom, R.W. (2006). Light absorption by carbonaceous particles: An investigative review. *Aerosol Sci. Technol.* 40: 27–67.

Burtscher, H., Baltensperger, U., Bukowiecki, N., Cohn, P., Hüglin, C., Mohr, M., Matter, U., Nyeki, S., Schmatloch, V., Streit, N. and Weingartner, E. (2001). Separation of volatile and non-volatile aerosol fractions by thermodesorption: Instrumental development and applications. *Aerosol Sci. Technol.* 32: 427–442.

Cao, J.J., Lee, S.C., Zhang, X.Y., Chow, J.C., An, Z.S., Ho, K.F., Watson, J.G., Fung, K., Wang, Y.Q. and Shen, Z.X. (2005). Characterization of airborne carbonate over a site near Asian dust source regions during spring 2002 and its climatic and environmental significance. *J. Geophys. Res.* 110: D03203.

Capes, G., Johnson, B., McFiggans, G., Williams, P.I., Haywood, J. and Coe, H. (2008). Aging of biomass burning aerosols over West Africa: Aircraft measurements of chemical composition, microphysical properties, and emission ratios. *J. Geophys. Res.* 113: D00C15.

Cazorla, A., Bahadur, R., Suski, K.J., Cahill, J.F., Chand, D., Schmid, B., Ramanathan, V. and Prather, K.A. (2013). Relating aerosol absorption due to soot, organic carbon, and dust to emission sources determined from in-situ chemical measurements. *Atmos. Chem. Phys.* 13: 9337–9350.

Chen, P., Kang, S., Li, C., Rupakheti, M., Yan, F., Li, Q., Ji, Z., Zhang, Q., Luo, W. and Sillanpää, M. (2015). Characteristics and sources of polycyclic aromatic hydrocarbons in atmospheric aerosols in the Kathmandu Valley, Nepal. *Sci. Total Environ.* 538: 86–92.

Chung, S.H. and Seinfeld, J.H. (2002). Global distribution and climate forcing of carbonaceous aerosols. *J. Geophys. Res.* 107: 4407.

Clarke, A.D. (1993). Atmospheric nuclei in the Pacific midtroposphere: Their nature, concentration, and evolution. *J. Geophys. Res.* 98: 20633–20647.

Cross, E.S., Onasch, T.B., Ahern, A., Wrobel, W., Slowik, J.G., Olfert, J., Lack, D.A., Massoli, P., Cappa, C.D., Schwarz, J.P., Spackman, J.R., Fahey, D.W., Sedlacek, A., Trimborn, A., Jayne, J.T., Freedman, A., Williams, L.R., Ng, N.L., Mazzoleni, C., Dubey, M., Brem, B., Kok, G., Subramanian, R., Freitag, S., Clarke, A., Thornhill, D., Marr, L.C., Kolb, C.E., Worsnop, D.R. and Davidovits, P. (2010). Soot particle studies—instrument inter-comparison—project overview. *Aerosol Sci. Technol.* 44: 592–611.

Dalton, T.P., Kerzee, J.K., Wang, B., Miller, M., Dieter, M.Z., Lorenz, J.N., Shertzer, H.G., Nebert, D.W. and Puga, A. (2001). Dioxin exposure is an environmental risk factor for ischemic heart disease. *Cardiovasc. Toxicol.* 1: 285–298.

Drinovec, L., Močnik, G., Zotter, P., Prévôt, A.S.H., Ruckstuhl, C., Coz, E., Rupakheti, M., Sciare, J., Müller, T., Wiedensohler, A. and Hansen, A.D.A. (2015). The "dual-spot" Aethalometer: An improved measurement of aerosol black carbon with real-time loading compensation. *Atmos. Meas. Tech.* 8: 1965–1979.

Dzubay, T.G., Stevens, R.K., Lewis, C.W., Hern, D.H., Courtney, W.J., Tesch, J.W. and Mason, M.A. (1982). Visibility and aerosol composition in Houston, Texas. *Environ. Sci. Technol.* 16: 514–525.

Ehhalt, D., Georgii, H.W., Warneck, P., Zellner, R., Mentel, T.F. and Sausen, R. (1999). *Global aspects of atmospheric chemistry*. Steinkopff, New York.

Ferry, G.V., Pueschel, R.F., Strawa, A.W., Kondo, Y., Howard, S.D., Verma, S., Mahoney, M.J., Bui, T.P., Hannan, J.R. and Fuelberg, H.E. (1999). Effects of aircraft on aerosol abundance in the upper troposphere. *Geophys. Res. Lett.* 26: 2399–2402.

Fierz, M., Vernooij, M.G.C. and Burtscher, H. (2007). An improved low-flow thermodenuder. *J. Aerosol Sci.* 38: 1163–1168.

Fuzzi, S., Andreae, M.O., Huebert, B.J., Kulmala, M., Bond, T.C., Boy, M., Doherty, S.J., Guenther, A., Kanakidou, M., Kawamura, K., Kerminen, V.M., Lohmann, U., Russell, L.M. and Pöschl, U. (2006). Critical assessment of the current state of scientific knowledge, terminology, and research needs concerning the role of organic aerosols in the atmosphere, climate, and global change. *Atmos. Chem. Phys.* 6: 2017–2038.

Gillespie, J.B. and Lindberg, J.D. (1992). Ultraviolet and visible imaginary refractive index of strongly absorbing atmospheric particulate matter. *Appl. Opt.* 31: 2112–2115.

Grimm, H. and Eatough, D.J. (2009). Aerosol measurement: The use of optical light scattering for the determination of particulate size distribution, and particulate mass, including the semi-volatile fraction. *J. Air Waste Manage. Assoc.* 59: 101–107.

Grover, B.D., Kleinman, M., Eatough, N.L., Eatough, D.J., Hopke, P.K., Long, R.W., Wilson, W.E., Meyer, M.B. and Ambs, J.L. (2005). Measurement of total $PM_{2.5}$ mass (nonvolatile plus semivolatile) with the Filter Dynamic Measurement System tapered element oscillating microbalance monitor. *J. Geophys. Res.* 11: D07S03.

Haywood, J.M. and Shine, K.P. (1997). Multi-spectral calculations of the direct radiative forcing of tropospheric sulphate and soot aerosols using a column model. *Q. J. R. Meteorolog. Soc.* 123: 1907–1930.

Hennigan, C.J., Sullivan, A.P., Fountoukis, C.I., Nenes, A., Hecobian, A., Vargas, O. and Peltier, R.E. (2008). On the volatility and production mechanisms of newly formed nitrate and water soluble organic aerosol in Mexico City. *Atmos. Chem. Phys.* 8: 3761–3768.

Hermann, M., Wehner, B., Bischof, O., Han, H.S., Krinke, T., Liu, W., Zerrath, A. and Wiedensohler, A. (2007). Particle counting efficiencies of new TSI condensation particle counters. *J. Aerosol Sci.* 38: 674–682.

Hogrefe, O., Lala, G.G., Frank, B.P., Schwab, J.J. and Demerjian, K.L. (2006). Field evaluation of a TSI 3034 Scanning Mobility Particle Sizer in New York City: Winter 2004 intensive campaign. *Aerosol Sci. Technol.* 40: 753–762.

Huang, B., Lei, C., Wei, C. and Zeng, G. (2014). Chlorinated volatile organic compounds (Cl-VOCs) in environment - sources, potential human health impacts, and current remediation technologies. *Environ. Int.* 71: 118–138.

Huffman, J.A., Docherty, K.S., Aiken, A.C., Cubison, M.J., Ulbrich, I.M., Decarlo, P.F. and Sueper, D. (2009). Chemically-resolved aerosol volatility measurements from two megacity field studies. *Atmos. Chem. Phys.* 9: 7161–7182.

Huffman, J.A., Ziemann, P.J., Jayne, J.T., Worsnop, D.R. and Jimenez, J.L. (2008). Development and characterization of a fast-stepping/scanning thermodenuder for chemically-resolved aerosol volatility measurements. *Aerosol Sci. Technol.* 42: 395–407.

Ishizaka, Y. and Adhikari, M. (2003). Composition of cloud condensation nuclei. *J. Geophys. Res.* 108: 4138.

Jennings, S.G., O'Dowd, C.D., Cooke, W.F., Sheridan, P.J. and Cachier, H. (1994). Volatility of elemental carbon. *Geophys. Res. Lett.* 21: 1719–1722.

Kampa, M. and Castanas, E. (2008). Human health effects of air pollution. *Environ. Pollut.* 151: 362–367.

Kim, B.M., Park, J.S., Kim, S.W., Kim, H., Jeon, H., Cho, C., Kim, J.H., Hong, S., Rupakheti, M., Panday, A.K., Park, R.J., Hong, J. and Yoon, S.C. (2015). Source apportionment of PM_{10} mass and particulate carbon in the Kathmandu Valley, Nepal. *Atmos. Environ.* 123: 190–199.

Kim, C.H., Choi, Y. and Ghim, Y.S. (2015). Characterization of volatilization of filter-sampled $PM_{2.5}$ semi-volatile inorganic ions using a backup filter and denuders. *Aerosol Air Qual.Res.* 15: 814–820.

Kirchstetter, T.W., Novakov, T. and Hobbs, P.V. (2004). Evidence that the spectral dependence of light absorption by aerosols is affected by organic carbon. *J. Geophys. Res.* 109: D21208.

Lerner, J.E.C., Kohajda, T., Aguilar, M.E., Massolo, L.A., Sánchez, E.Y., Porta, A.A., Opitz, P., Wichmann, G., Herbarth, O. and Mueller, A. (2014). Improvement of health risk factors after reduction of VOC concentrations in industrial and urban areas. *Environ. Sci. Pollut. Res.* 21: 9676–9688.

Lack, D.A. and Cappa, C.D. (2010). Impact of brown and

clear carbon on light absorption enhancement, single scatter albedo and absorption wavelength dependence of black carbon. *Atmos. Chem. Phys.* 10: 4207–4220.

Lack, D.A., Richardson, M.S., Law, D., Langridge, J.M., Cappa, C.D., McLaughlin, R.J. and Murphy, D.M. (2012). Aircraft instrument for comprehensive characterization of aerosol optical properties, Part 2: Black and brown carbon absorption and absorption enhancement measured with photo acoustic spectroscopy. *Aerosol Sci. Technol.* 46: 555–568.

Lang-Yona, N., Abo-Riziq, A., Erlick, C., Segre, E., Trainic, M. and Rudich, Y. (2010). Interaction of internally mixed aerosols with light. *Phys. Chem. Chem. Phys.* 12: 21–31.

Lee, B.H., Kostenidou, E., Hildebrandt, L., Riipinen, I., Engelhart, G.J., Mohr, C., DeCarlo, P.F., Mihalopoulos, N., Prevot, A.S.H., Baltensperger, U. and Pandis, S.N. (2010). Measurement of the ambient organic aerosol volatility distribution: Application during the Finokalia Aerosol Measurement Experiment (FAME-2008). *Atmos. Chem. Phys.* 10: 12149–12160.

Lim, S., Lee, M., Kim, S.W., Yoon, S.C., Lee, G. and Lee, Y.J. (2014). Absorption and scattering properties of organic carbon versus sulfate dominant aerosols at Gosan climate observatory in Northeast Asia. *Atmos. Chem. Phys.* 14: 7781–7793.

Lin, G. (2013). *Global modeling of secondary organic aerosol formation: From atmospheric chemistry to climate*. University of Michigan.

Lindberg, J.D., Douglass, R.E. and Garvey, D.M. (1993). Carbon and the optical properties of atmospheric dust. *Appl. Opt.* 32: 6077.

Madl, P., Yip, M., Ristovski, Z., Morawska, L. and Hofmann, W. (2003). Redesign of a thermodenuder and assessment of its performance. Division of Molecular Biology – Department of Physics and Biophysics Dosimetry and Modelling Working Group, University of Salzburg, 3065.

Mauderly, J.L. and Chow, J.C. (2008). Health effects of organic aerosols. *Inhalation Toxicol.* 20: 257–288.

Mishra, S.K. and Tripathi, S.N. (2008). Modeling optical properties of mineral dust over the Indian Desert. *J. Geophys. Res.* 113: D23201.

Murugavel, P. and Chate, D.M. (2011). Volatile properties of atmospheric aerosols during nucleation events at Pune, India. *J. Earth Syst. Sci.* 120: 347–357.

Orsini, D.A., Wiedensohler, A., Stratmann, F. and Covert, D.S. (1999). A new volatility tandem differential mobility analyzer to measure the volatile sulfuric acid aerosol fraction. *J. Atmos. Oceanic Technol.* 16: 760–772.

Panday, A.K. and Prinn, R.G. (2009). Diurnal cycle of air pollution in the Kathmandu Valley, Nepal: Observations. *J. Geophys. Res.* 114: D09305.

Panday, A.K., Prinn, R.G. and Schär, C. (2009a). Diurnal cycle of air pollution in the Kathmandu Valley, Nepal: 2. Modeling results. *J. Geophys. Res.* 114: D21308.

Petzold, A., Ogren, J.A., Fiebig, M., Laj, P., Li, S.M., Baltensperger, U., Holzer-Popp, T., Kinne, S., Pappalardo, G., Sugimoto, N., Wehrli, C., Wiedensohler, A. and Zhang, X.Y. (2013). Recommendations for reporting "black carbon" measurements. *Atmos. Chem. Phys.* 13: 8365–8379.

Philippin, S., Wiedensohler, A. and Stratmann, F. (2004). Measurements of non-volatile fractions of pollution aerosols with an eight-tube volatility tandem differential mobility analyzer (VTDMA-8). *J. Aerosol Sci.* 35: 185–203.

Pöschl, U. (2005). Atmospheric aerosols: Composition, transformation, climate and health effects. *Angew. Chem. Int. Ed*. 44: 7520–7540.

Putero, D., Cristofanelli, P., Marinoni, A., Adhikary, B., Duchi, R., Shrestha, S.D., Verza, G.P., Landi, T.C., Calzolari, F., Busetto, M., Agrillo, G., Biancofiore, F., Di Carlo, P., Panday, A.K., Rupakheti, M. and Bonasoni, P. (2015). Seasonal variation of ozone and black carbon observed at Paknajol, an urban site in the Kathmandu Valley, Nepal. *Atmos. Chem. Phys.* 15: 13957–13971.

Regmi, R.P. and Maharjan, S. (2015). Trapped mountain wave excitations over the Kathmandu valley, Nepal. *Asia-Pac. J. Atmos. Sci.* 51: 303–309.

Robinson, A.L., Donahue, N.M., Shrivastava, M.K., Weitkamp, E.A., Sage, A.M., Grieshop, A.P., Lane, T.E., Pierce, J.R. and Pandis, S.N. (2007). Rethinking organic aerosols: Semivolatile emissions and photochemical aging. *Science* 315: 1259–1262.

Ronai, Z.A., Gradia, S., El-Bayoumy, K., Amin, S. and Hecht, S.S. (1994). Contrasting incidence of ras mutations in rat mammary and mouse skin tumors induced by *anti*-benzo[c]phenanthrene-3,4-diol-1,2-epoxide. *Carcinogenesis* 15: 2113–2116.

Sarigiannis, D.A., Kermenidou, M., Nikolaki, S., Zikopoulos, D. and Karakitsios, S.P. (2015). Mortality and morbidity attributed to aerosol and gaseous emissions from biomass use for space heating. *Aerosol Air Qual. Res.* 15: 2496–2507.

Sarkar, C., Sinha, V., Sinha, B., Panday, A.K., Rupakheti, M. and Lawrence, M.G. (2017). Source apportionment of NMVOCs in the Kathmandu Valley during the SusKat-ABC international field campaign using positive matrix factorization. *Atmos. Chem. Phys.* 17: 8129–8156.

Schmid, O., Eimer, B., Hagen, D.E. and Whitefield, P.D. (2002). Investigation of volatility method for measuring aqueous sulfuric acid on mixed aerosols. *Aerosol Sci. Technol.* 36: 877–889.

Schnaiter, M. (2005). Absorption amplification of black carbon internally mixed with secondary organic aerosol. *J. Geophys. Res.* 110: D19204.

Seinfeld, J.H. and Pandis, S.N. (2006). *Atmospheric chemistry and physics: From air pollution to climate change*. 2nd Edition, John Wiley & Sons, New York.

Shakya, K.M., Ziemba, L.D. and Griffin, R.J. (2010). Characteristics and sources of carbonaceous, ionic, and isotopic species of wintertime atmospheric aerosols in Kathmandu valley, Nepal. *Aerosol Air Qual. Res.* 10: 219–230.

Shakya, K.M., Rupakheti, M., Shahi, A., Maskey, R., Pradhan, B., Panday, A., Puppala, S.P., Lawrence, M. and Peltier, R.E. (2017). Near-road sampling of $PM_{2.5}$, BC, and fine-particle chemical components in Kathmandu

Valley, Nepal. *Atmos. Chem. Phys.* 17: 6503–6516.

Shiraiwa, M., Kondo, Y., Iwamoto, T. and Kita, K. (2010). Amplification of light absorption of black carbon by organic coating. *Aerosol Sci. Technol.* 44: 46–54.

Shrestha, R., Kim, S.W., Yoon, S.C. and Kim, J. H. (2014). Attribution of aerosol light absorption to black carbon and volatile aerosols. *Environ. Monit. Assess.* 186: 4743–4751.

Singh, A., Rajput, P., Sharma, D., Sarin, M.M. and Singh, D. (2014). Black carbon and elemental carbon from postharvest agricultural-waste burning emissions in the Indo-Gangetic plain. *Adv. Meteorol.* 2014: 179301.

Slowik, J.G., Cross, E.S., Han, J.H., Davidovits, P., Onasch, T.B., Jayne, J.T., Williams, L.R., Canagaratna, M.R., Worsnop, D.R., Chakrabarty, R.K., Moosmüller, H., Arnott, W.P., Schwarz, J.P., Gao, R.S., Fahey, D.W., Kok, G.L. and Petzold, A. (2007). An inter-comparison of instruments measuring black carbon content of soot particles. *Aerosol Sci. Technol.* 41: 295–314.

Snyder, D.C. and Schauer, J.J. (2007). An inter-comparison of two black carbon aerosol instruments and a semi-continuous elemental carbon instrument in the urban environment. *Aerosol Sci. Technol.* 41: 463–474.

Sokolik, I.N. and Toon, O.B. (1999). Incorporation of mineralogical composition into models of the radiative properties of mineral aerosol from UV to IR wavelengths. *J. Geophys. Res.* 104: 9423–9444.

Stanier, C.O., Khlystov, A.Y., Chan, W.R., Mandiro, M. and Pandis, S.N. (2004). A method for the in situ measurement of fine aerosol water content of ambient aerosols: The dry-ambient aerosol size spectrometer (DAASS). *Aerosol Sci. Technol.* 38: 215–228.

Stevanovic, S., Miljevic, B., Madl, P., Clifford, S. and Ristovski, Z. (2015). Characterisation of a commercially available thermodenuder and diffusion drier for ultrafine particles losses. *Aerosol Air Qual. Res.* 15: 357–363.

Valenzuela, A., Olmo, F.J., Lyamani, H., Antón, M., Titos, G., Cazorla, A. and Alados-Arboledas, L. (2015). Aerosol scattering and absorption Angström exponents as indicators of dust and dust-free days over Granada (Spain). *Atmos. Res*. 154: 1–13.

Warneck, P. (1999). *Chemistry of the natural atmosphere*. Academic Press, New York.

Yu, H., Kaufman, Y.J., Chin, M., Feingold, G., Remer, L.A., Anderson, T.L., Balkanski, Y., Bellouin, N., Boucher, O., Christopher, S., DeCola, P., Kahn, R., Koch, D., Loeb, N., Reddy, M.S., Schulz, M., Takemura, T. and Zhou, M. (2006). A review of measurement-based assessments of the aerosol direct radiative effect and forcing. *Atmos. Chem. Phys.* 6: 613–666.

Zhang, R., Khalizov, A.F., Pagels, J., Zhang, D., Xue, H. and McMurry, P.H. (2008). Variability in morphology, hygroscopicity, and optical properties of soot aerosols during atmospheric processing. *Proc. Natl. Acad. Sci. U.S.A.* 105: 10291–10296.

Received for review, December 3, 2017
Revised, December 30, 2017
Accepted, December 31, 2017